A&A 382, 1106–1117 (2002)
DOI: 10.1051/0004-6361:20011705
© ESO 2002

Astronomy & Astrophysics

Fe XIII line intensities in solar plasmas observed by SERTS

E. Landi[1,2,⋆]

[1] Naval Research Laboratory, Washington DC, 20375, USA
[2] Max-Planck-Institut für Aeronomie, 37191 Katlenburg-Lindau, Germany

Received 25 September 2001 / Accepted 23 November 2001

Abstract. Extreme-Ultraviolet spectral observations of Fe XIII lines, obtained during the 1989 and 1995 flights of the SERTS instrument, are compared with line emissivities derived from two different sets of atomic data and transition probabilities. One dataset is based upon calculations involving the Close-Coupling approximation, and the other is based upon the Distorted Wave approximation. Emission line ratios that are insensitive to density and temperature are used to assess both the quality of the transition rates and possible line blending. Density-sensitive line ratios are used to measure the electron density. The comparison between the observed and the theoretical line ratios yields a set of lines, free of blends, that is recommended for plasma diagnostic studies. Both theoretical datasets yield the same set of lines, which includes wavelengths of 200.02, 201.13, 202.04, 203.16, 203.82, 209.67, 209.92, 256.43, 312.17, 312.87, 320.80, 348.18, 359.64 and 413.00 Å. Electron densities derived from line ratios calculated with each theoretical dataset differ by a factor $\simeq$2, comparable to the scatter in density measurements from other ions formed at similar temperatures, as well as to the uncertainties on some of the individual density measurements. This precludes determining which of the two datasets is more accurate. Ambiguities in a few of the line intensity ratios suggest that new, more accurate calculations of transition rates are needed.

Key words. Sun: corona – Sun: transition region – Sun: UV radiation – line: profiles

1. Introduction

Fe XIII lines are prominent in EUV spectra recorded from solar and stellar coronae. In particular Fe XIII includes sets of well resolved density sensitive line ratios. Some twenty years ago Fe XIII lines from solar active regions and flares observed by Skylab were analyzed by Dere et al. (1979) and Dere (1982); more recently several authors have used the same lines from Solar EUV Rocket Telescope and Spectrograph (SERTS) observations of quiet Sun and active regions (Brosius et al. 1996, 1998, 2000). Fe XIII lines observed by the Coronal Diagnostic Spectrometer (CDS) on board of the Solar and Heliospheric Observatory (SOHO) spacecraft have been studied by O'Shea et al. (1998), Landi & Landini (1998), Mason et al. (1999). Lines from Fe XIII have also been analyzed in the spectra of the stars Alpha Cen and Procyon from the Extreme Ultraviolet Explorer (EUVE) satellite (Keenan et al. 1995). In all cases, these lines have proved excellent tools for density diagnostics at coronal temperatures.

The importance of Fe XIII for plasma diagnostics has triggered a number of independent calculations of Fe^{12+} atomic structure, collisional cross-sections and transition probabilities. These calculations were carried out using various approximations, and have led to differences in the predicted line emissivities. Distorted Wave calculations were performed by Flower (1971), Flower & Pineau des Forêts (1973), Flower & Nussbaumer (1974), Fawcett & Mason (1989); Close-Coupling computations were carried out by Tayal (1995) and Gupta & Tayal (1998); Tayal (2000) extended the calculation of Gupta & Tayal (1998) to the $1 \times 10^4 - 5 \times 10^5$ K temperature range. Agreement between the results of the latest calculations is generally acceptable, with the exception of a few transitions, as noted by Gupta & Tayal (1998).

However, solar observations with Solar EUV Rocket Telescope and Spectrograph (SERTS) carried out in 1989 (Thomas & Neupert 1994; Young et al. 1998: SERTS-89) have shown that some problems are found when comparing many of the observed Fe XIII lines with theoretical line emissivity calculations. Similar results have been also found by Landi & Landini (1997) analyzing Fe XIII line intensities from portions of the SERTS-89 slit. Young et al. (1998) report that some density-insensitive line ratios do not agree with theoretical predictions from the CHIANTI database (Dere et al. 1997), and that some of the density diagnostic ratios provide N_e values either much lower or much higher than most of the other Fe XIII or other ions' line ratios. Discrepancies among electron densities from

⋆ e-mail: landi@poppeo.nrl.navy.mil

Article published by EDP Sciences and available at http://www.aanda.org or http://dx.doi.org/10.1051/0004-6361:20011705

several Fe XIII ratios have also been found by Brickhouse et al. (1995), who also point out several inconsistencies between theoretical and observed intensities for several Fe XIII lines. Using observed intensities as a guide, Landi & Landini (1997) noticed that the theoretical intensities of Fe XIII lines having wavelengths shorter than 300 Å appear to be too intense in comparison to lines having wavelengths longer than 300 Å.

The aim of the present work is to investigate these discrepancies, by comparing Fe XIII line intensities, observed by SERTS during the 1989 (hereafter SERTS-89) and 1995 flights (Brosius et al. 1998, hereafter SERTS-95), with theoretical predictions obtained with two different datasets of atomic parameters and collisional transition probabilities. One of these datasets was calculated using the Distorted Wave approximation (Fawcett & Mason 1989), and the other using the Close-Coupling approach (Tayal & Gupta 1998). The present analysis allows us to:

1. assess which Fe XIII lines are affected by blending problems and which ones are affected by atomic physics problems;
2. select a set of recommended lines for plasma diagnostic purposes;
3. assess the quality of the two theoretical datasets and recommend the most reliable one.

The paper is structured as follows: in Sect. 2 the two theoretical calculations for the Fe XIII atomic data, collisional cross-sections and transition probabilities are described and compared. Section 3 introduces the observations and in Sect. 4 observed and theoretical line ratios are compared. The results are discussed in Sect. 5.

2. Atomic physics calculations

In the present work the Fe XIII atomic parameters and transition probabilities are taken from two different versions of the CHIANTI database. The Distorted Wave dataset comes from CHIANTI version 1 (Dere et al. 1997) and the Close-Coupling data are taken from CHIANTI version 3 (Dere et al. 2001). Below a few details of the datasets are given.

2.1. The Distorted Wave calculation

Fawcett & Mason (1989) adopted the Distorted Wave approximation (Eissner & Seaton 1972) with a modified set of Slater parameters for the target eigenfunctions.

Fawcett & Mason (1989) argue that the use of atomic structure codes for ab initio calculation of complex ions does not yield accurate results because these codes fail to properly take into account the interactions with high energy configurations. Consequently the resulting energy levels and oscillator strengths are often different from the observed values. Also, these inaccuracies are passed into the calculation of collision parameters, thus leading to inaccurate collision strengths. They propose to use semiempirical optimized Slater parameters for the ion eigenfunctions. Target eigenfunctions are calculated ab initio using the SUPERSTRUCTURE program (Eissner et al. 1974); however, as soon as Slater parameters are calculated by this program, they are substituted with a set of optimized values. These are obtained by a least-square-fitting routine developed by Cowan (1981), starting from the set of Slater parameters obtained with an Hartree-Fock-Relativistic (HFR) atomic structure code (Fawcett 1987 and references therein). The initial HFR Slater parameters are optimized by minimizing the differences between HFR energy levels and observed energy levels. The ion eigenfunctions obtained by making use of the optimized Slater parameters are then used throughout the calculation of radiative data with SUPERSTRUCTURE and of the collisional transition probabilities.

The Fawcett & Mason (1989) atomic model includes the $3s^23p^2$ ground configuration and the $3s3p^3$ and $3s^23p3d$ excited configurations, corresponding to 27 fine structure energy levels. They include six configurations in their calculations, and provide collision strengths for 3 values of the incident electron energy: 15, 30 and 45 Rydberg. It is important to note that Fawcett & Mason (1989) provide collision strengths only for excitations out of the ground configuration, so that excitations out of metastable levels (as the $3s^23p3d\ ^3F_4$ level) are not taken into account. Fits of these collision strengths are provided by Mason (1994).

CHIANTI adopts radiative transition probabilities from a SUPERSTRUCTURE calculation obtained from a 24-configuration model; most importantly, these calculations include radiative transition probabilities to populate and de-populate the $3s^23p3d\ ^3F_4$ metastable level.

This dataset will be referred to as FAWCETT in the rest of the present work.

2.2. The Close-Coupling calculation

The Gupta & Tayal (1998) dataset represents an improvement relative to the Tayal (1995) Close-Coupling calculation, and provides data for the same configurations considered by Fawcett & Mason (1989). The only difference is in the $3s3p^3\ ^5S_2$ level, for which Gupta & Tayal (1998) do not publish any result.

Tayal (1995) included in his calculation configuration-interaction effects only within the $n = 3$ complex; Gupta & Tayal (1998) increase the number of target states and include correlation effects also from the 4f orbital. The total number of terms used in the Gupta & Tayal (1998) calculation to represent the 14 LS levels are 70, arising from the n = 1, 2, 3 and 4f orbitals. A semirelativistic Close-Coupling method is used to calculate collision strengths for transitions within the ground configuration, and from the ground to the first two excited configurations. The "effective" collision strengths were obtained by averaging the collision strengths with a Maxwellian distribution of electron energies and provided for temperatures between 5×10^5 and 5×10^6 K. Since no data is provided for the metastable $3s3p^{35}S_2$ level, CHIANTI V.3 includes the

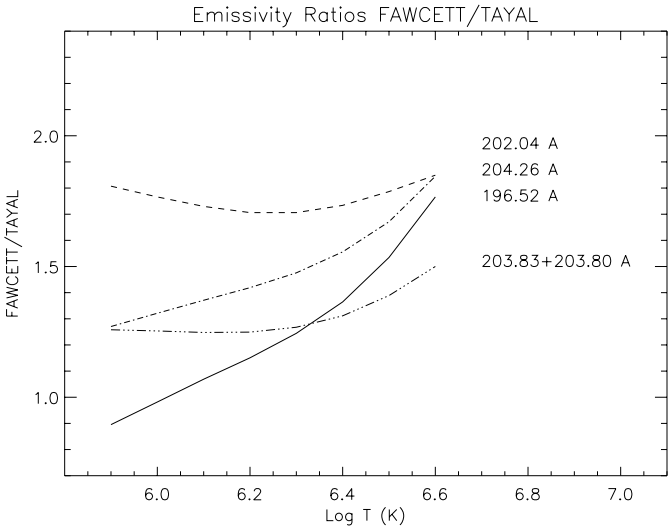

Fig. 1. Ratios of line emissivities from the TAYAL and FAWCETT datasets for selected $3s^23p^2$–$3s^23p3d$ transitions, as a function of electron temperature. The curves have been calculated at $Ne = 10^{10}$ cm^{-3}.

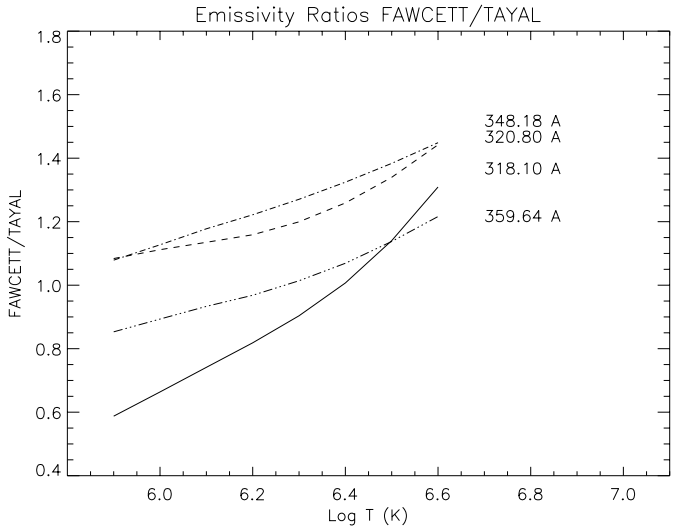

Fig. 2. Ratios of line emissivities from the TAYAL and FAWCETT datasets for selected $3s^23p^2$–$3s3p^3$ transitions, as a function of electron temperature. The curves have been calculated at $Ne = 10^{10}$ cm^{-3}.

Fawcett & Mason (1989) collisional data for transitions involving this level.

Since in the present work we are interested in active region spectra, formed at temperatures in excess of one million degrees, we consider only the Gupta & Tayal (1998) data, and not the lower-temperature collision rates calculated by Tayal (2000).

Radiative transition probabilities are the same as in CHIANTI version 1. It is important to note that also this dataset does not take into account excitations from metastable levels (such as the $3s^23p3d\ ^3F_4$ level).

This dataset will be referred to as TAYAL in the rest of the present work.

2.3. Comparison of results

Gupta & Tayal (1998) report that their collision strengths are lower than the Fawcett & Mason (1989) for most of the allowed transitions. The authors suggest that this might be due to the use of the Bethe approximation for calculating the contributions of high-L partial waves: Fawcett & Mason (1989) use the Bethe approximation starting from total orbital angular momentum $L = 8$, while Gupta & Tayal (1998) use the Close-Coupling approximation up to total angular momentum $J = 22.5$. The Bethe approximation may overestimate the collision strengths for low-L partial waves (Tayal 1995), and this could be the cause of at least part of the discrepancy. It is expected that these differences might lead to significant effects on line emissivities and on diagnostic results.

Figures 1 to 4 show the ratios between line emissivities from the TAYAL and FAWCETT datasets for a few selected lines originated from both excited configurations.

These lines are among the most intense transitions in the Fe XIII spectrum and are commonly used in plasma

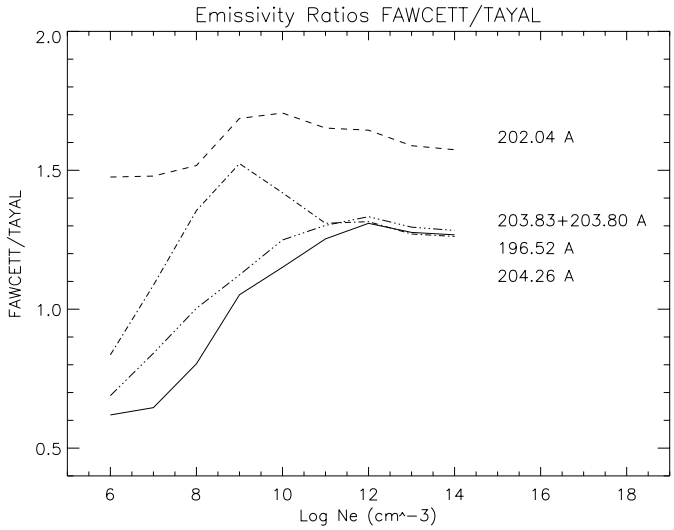

Fig. 3. Ratios of line emissivities from the TAYAL and FAWCETT datasets for selected $3s^23p^2$–$3s^23p3d$ transitions, as a function of electron density. The curves have been calculated at $T = 1.6 \times 10^6$ K, the temperature of maximum abundance of Fe XIII (Mazzotta et al. 1998).

diagnostic studies. The comparison is carried out both as a function of temperature and density. It is possible to see that, as expected, the two datasets lead to substantially different results, and differences, that can rise up to a factor 2.5, depend on both electron density and temperature. At higher densities FAWCETT-based emissivities tend to be higher than those given by the TAYAL dataset.

Due to the size of the differences in the emissivities, huge effects are expected to occur on the line ratios. A few examples are displayed in Figs. 5 and 6, where line ratios calculated from the TAYAL and FAWCETT datasets are compared; most of these ratios will be compared with observations in Sect. 4. Figures 5 and 6 show that although

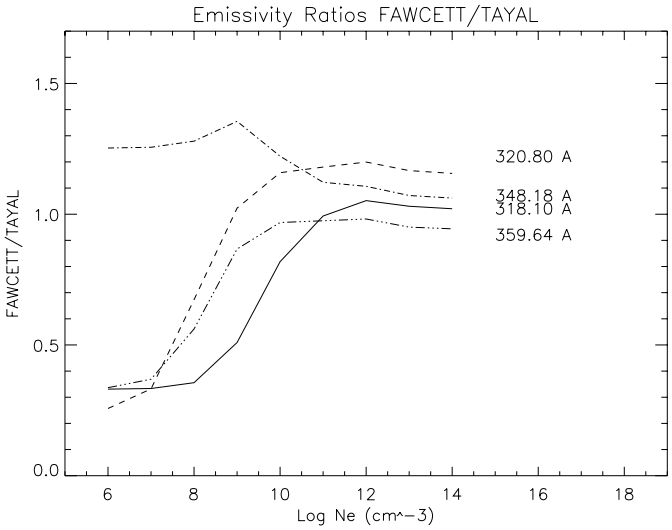

Fig. 4. Ratios of line emissivities from the TAYAL and FAWCETT datasets for selected $3s^2 3p^2$–$3s3p^3$ transitions, as a function of electron density. The curves have been calculated at $T = 1.6 \times 10^6$ K, the temperature of maximum abundance of Fe XIII (Mazzotta et al. 1998).

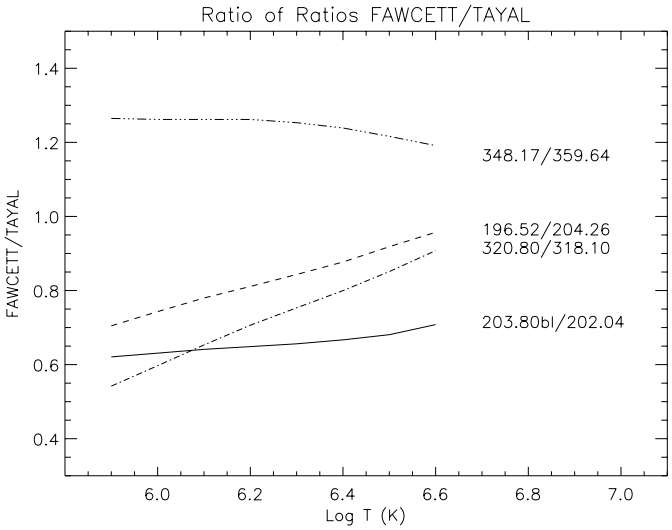

Fig. 5. Ratios of line emissivity ratios from the TAYAL and FAWCETT datasets for selected line pairs, as a function of the electron temperature. The emissivity of the 203.82 Å line has been obtained summing the emissivities of the two blending lines.

differences between the FAWCETT and TAYAL datasets are only weakly temperature dependent, their density sensitivity is strong enough to change plasma diagnostic results virtually at all the density regimes typical of solar and stellar coronae.

While a detailed comparison of excitation rates, line emissivities and theoretical ratios obtained from the FAWCETT and TAYAL datasets is beyond the scope of the present work, these few examples clearly show that differences in the theoretical emissivities result in significant effects on plasma diagnostic when they are compared with observations. It is important, then, to assess which

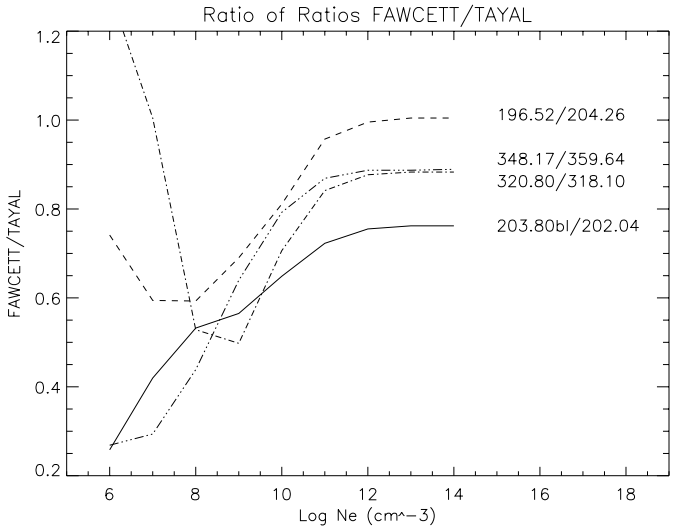

Fig. 6. Ratios of line emissivity ratios from the TAYAL and FAWCETT datasets for selected line pairs, as a function of the electron density. The emissivity of the 203.82 Å line has been obtained summing the emissivities of the two blending lines.

of the TAYAL and FAWCETT datasets is more accurate and can be recommended for further plasma diagnostic studies.

3. SERTS observations

The Solar EUV Rocket Telescope and Spectrograph (SERTS) has been flown on several occasions, and has provided imaged EUV spectra of the Sun with the highest spectral resolution ever achieved. In the present work we focus our attention to the Fe XIII line intensities from the 1989 flight (SERTS-89) and from the 1995 flight (SERTS-95).

3.1. SERTS 1989 flight

The SERTS version flown on 1989 covered the 235–450 Å wavelength region in first order and the 170–225 Å range in second order, and 23 Fe XIII lines were reported. The field of view included mostly active region plasma in an area of around $7'' \times 276''$, although a small subflare was imaged on the central part of the slit.

The complete spectrum, obtained by averaging the emission over the whole slit length, was published by Thomas & Neupert (1994), with a few revisions from Young et al. (1998). The observed line intensities are reported in Table 1. It is to be noted that Young et al. (1998) proposed a correction to the SERTS-89 intensity calibration in the 400–450 Å range, which affects the intensity of the 413.00 Å line: this correction has been taken into account in the present work.

Subsequent re-evaluation of the absolute calibration scale for SERTS-89 indicates that all intensities reported in the catalogue published by Thomas & Neupert (1994) should be increased by a factor of 1.24. However since we

Table 1. Fe XIII fluxes from the SERTS-89 and SERTS-95 observations. SERTS-89 intensity for the 413.00 Å line has been corrected according to Young et al. (1998). Intensities are in erg cm^{-2} s^{-1} sr−1.

Wvl.(Å)	SERTS-95	SERTS-89	Transition
196.52	135 ± 33.4		$3s^23p^2\ ^1D_2$–$3s^23p3d\ ^1F_3$
200.02	304 ± 36.7		$3s^23p^2\ ^3P_1$–$3s^23p3d\ ^3D_2$
201.12	470 ± 60.6	394 ± 137.0	$3s^23p^2\ ^3P_1$–$3s^23p3d\ ^3D_1$
202.04	1210 ± 138.0	646 ± 109.0	$3s^23p^2\ ^3P_0$–$3s^23p3d\ ^3P_1$
203.16	154 ± 24.2		$3s^23p^2\ ^3P_1$–$3s^23p3d\ ^3P_0$
203.82	1930 ± 238.0	1060 ± 158.0	$3s^23p^2\ ^3P_2$–$3s^23p3d\ ^3D_{2,3}$
204.26	195 ± 29.7	141 ± 41.0	$3s^23p^2\ ^3P_1$–$3s^23p3d\ ^1D_2$
204.95	267 ± 44.5	348 ± 93.0	$3s^23p^2\ ^3P_2$–$3s^23p3d\ ^3D_1$
209.62	210 ± 33.1	93.7 ± 51.0	$3s^23p^2\ ^3P_1$–$3s^23p3d\ ^3P_2$
209.91	225 ± 43.6		$3s^23p^2\ ^3P_2$–$3s^23p3d\ ^3P_1$
213.76	91.7 ± 20.6	58.3 ± 28.0	$3s^23p^2\ ^3P_2$–$3s^23p3d\ ^3P_2$
216.90	53.7 ± 16.3		$3s^23p^2\ ^1D_2$–$3s^23p3d\ ^3D_{2,3}$
221.81	218 ± 32.5	152 ± 47.0	$3s^23p^2\ ^1D_2$–$3s^23p3d\ ^1D_2$
240.69	160 ± 66.2	148 ± 61.0	$3s^23p^2\ ^3P_0$–$3s3p^3\ ^3S_1$
246.19	246 ± 47.4	160 ± 48.0	$3s^23p^2\ ^3P_1$–$3s3p^3\ ^3S_1$
251.94	332 ± 65.0	364 ± 55.0	$3s^23p^2\ ^3P_2$–$3s3p^3\ ^3S_1$
256.43		133 ± 51.0	$3s^23p^2\ ^1D_2$–$3s3p^3\ ^1P_1$
311.56		40.8 ± 10.9	$3s^23p^2\ ^3P_1$–$3s3p^3\ ^3P_2$
312.17	172 ± 33.8	85.9 ± 12.3	$3s^23p^2\ ^3P_1$–$3s3p^3\ ^3P_1$
312.87		47.6 ± 13.7	$3s^23p^2\ ^3P_1$–$3s3p^3\ ^3P_0$
318.10	112 ± 42.8	96.0 ± 13.9	$3s^23p^2\ ^1D_2$–$3s3p^3\ ^1D_2$
320.80	195 ± 57.8	172 ± 22.0	$3s^23p^2\ ^3P_2$–$3s3p^3\ ^3P_2$
321.46		32.9 ± 7.4	$3s^23p^2\ ^3P_2$–$3s3p^3\ ^3P_1$
348.18		128 ± 15.3	$3s^23p^2\ ^3P_0$–$3s3p^3\ ^3D_1$
359.64		147 ± 16.9	$3s^23p^2\ ^3P_1$–$3s3p^3\ ^3D_2$
359.83		22.4 ± 4.4	$3s^23p^2\ ^3P_1$–$3s3p^3\ ^3D_1$
368.16		128 ± 24.0	$3s^23p^2\ ^3P_2$–$3s3p^3\ ^3D_3$
413.00		6.0 ± 1.6	$3s^23p^2\ ^1D_2$–$3s3p^3\ ^3D_3$

are interested only in relative values, the original intensity scale is still used in the present work.

3.2. SERTS 1995 flight

The 1995 SERTS configuration included a multilayer coated toroidal diffraction grating that enhanced the instrumental sensitivity in the second order range (171–225 Å). The spectral resolution of the instrument was ≃30 mÅ in second order and ≃55 mÅ in first order. Due to the enhanced sensitivity at second order wavelengths, the SERTS-95 spectrum represents the highest quality observation of the Sun in the 171–225 Å spectral range ever obtained. Including the first order lines, a total of 20 Fe XIII lines were recorded by the instrument and reported by Brosius et al. (1998).

The relative intensity calibration of the instrument was obtained by means of comparison between a selection of observed line ratios and theoretical predictions from CHIANTI (Dere et al. 1997) as described by Brosius et al. (1998). The observed intensities are reported in Table 1.

The 1995 flight observed spectra from the NOAA active region 7870, although observations of quiet Sun have also been carried out. Due to the stronger signal-to-noise, only the active region spectrum is considered in the present study.

4. Comparison with observations

The present comparison is divided in three steps. Firstly, the ratios involving lines from the $3s^23p3d$ configurations only are compared with observations, in order to select a set of lines free of blending or atomic physics problems. In the second step, the same exercise is repeated with ratios involving lines from the $3s3p^3$ transition only. In the last step, we will compare ratios involving one $3s^23p3d$ line and one $3s3p^3$ line, using only those transitions that proved to be reliable in the previous two steps.

In order to take into account any residual density dependence in theoretical density-insensitive ratios, these were calculated as the average of their values at 10^8, 10^9, 10^{10}, 10^{11} and 10^{12} cm^{-3}. The standard deviation (1σ) of this average is taken as the uncertainty of the averaged value.

The density values measured during this analysis will be compared with measurements carried out in earlier studies on the same datasets we are considering, obtained by using density sensitive line pairs from other ions, formed at temperatures close to the Fe XIII temperature of formation. Densities from ions whose maximum abundance temperature is within 0.15 dex of the Fe XIII value (Log T = 6.20 – Mazzotta et al. 1998) are considered, with the exception of results obtained with

Table 2. Density measurements for the SERTS-89 and SERTS-95 active regions obtained from ions formed at similar temperatures than Fe XIII. Measurements come from Brosius et al. (1998) (SERTS-95) and Young et al. (1998) (SERTS-89). Fe XIII abundance peaks at Log $T = 6.2$ (Mazzotta et al. 1998).

Ion	Log T_M	Ratio	SERTS-95	SERTS-89
Fe XI	6.07	349/352		$9.2^{+0.3}_{-0.4}$
		184/182	$9.33^{+0.3}_{-0.4}$	
		184/188	$9.54^{+0.2}_{-0.3}$	
Si X	6.12	356/347		9.1 ± 0.3
Si XI	6.20	365/303		9.2 ± 0.2
S XI	6.24	246/247		$9.0^{+0.4}_{-0.9}$
Fe XIV	6.27	219/211	9.4 ± 0.10	9.5 ± 0.1
		353/334		9.5 ± 0.1
S XII	6.31	299/288		$9.5^{+0.2}_{-0.3}$
Fe XV	6.32	321/327		$9.4^{+0.3}_{-0.4}$

Fe XII line ratios: since atomic physics problems have been found in this ion by Binello et al. (2001), their values (Log $N_e \simeq 10.0$ cm^{-3}) are considered inaccurate. Density measurements from SERTS-89 and SERTS-95 studies by Young et al. (1998) and Brosius et al. (1998) are reported in Table 2. In the case of Fe XIV, Young et al. (1998) measurements have been replaced with densities obtained with the Storey et al. (2000) electron excitation rates, not available to Young et al. (1998).

The SERTS-95 measurements seem to cluster more compactly at Log $N_e \simeq 9.40$ (Log N_e in cm^{-3}); SERTS-89 densities present a wider scatter, and are in the range $9.0 <$ Log $N_e < 9.5$. Despite the fact that these densities are measured using line ratios of several different ions, they are remarkably consistent with each other, giving confidence in the overall accuracy of these measurements. It is expected that the Fe XIII lines will provide density values similar to those in Table 2. For this reason, a comparison between Fe XIII densities and those in Table 2 can help in discriminating which of the two theoretical datasets is more reliable, in case they provide different values of the electron density.

4.1. $3s^2\,3p3d$ lines

The strongest transitions between the ground and the $3s^23p3d$ configuration fall in the 170–240 Å wavelength range, and so they were observed with greater accuracy during the SERTS-95 flight. Also the SERTS-89 flight has recorded some of the strongest $3s^23p^2$–$3s^23p3d$ lines as second order lines, but their uncertainties are greater, some of them are blended with first order lines and moreover the SERTS-89 intensity calibration has been found to be uncertain by Young et al. (1998): for this reason we consider the SERTS-89 data only to confirm the results from SERTS-95 line intensities.

Branching ratios and mildly density sensitive ratios are displayed in Table 3. The degree of density sensitivity of the latter sometimes is different in the TAYAL and FAWCETT datasets, like for example the 209.63/204.26 and the 213.76/204.26 ratios. Experimental SERTS-89 ratios agree with the SERTS-95 ones within the uncertainties. For these, the SERTS-95 line intensities are considered to be more accurate.

Of all the theoretical branching ratios, only the 209.92/202.04 shows agreement with observations; the SERTS-89 value for the 209.67/213.76 ratio owes his agreement only to the very large uncertianties. The 204.26/221.83 observed ratio is higher than its theoretical value, but this is not probably due to a blend affecting the 204.26 Å line: the 209.67/204.26 ratio agrees nicely with its predicted value. The ratios involving the 221.81 Å are only in agreement with the TAYAL values, and not the FAWCETT ones, although in all cases the experimental value is higher than expected. Although it seems that the discrepancy observed in the 204.26/221.83 ratio is mostly due to the 221.83 Å line, a definitive conclusion cannot be reached. The high observed value of the 209.67/213.76 ratio is due to the 213.76 Å, whose theoretical intensity seems to be overestimated as witnessed by the other ratios involving the 213.76 line, while the 209.67 Å line gives no problems. The lack of density insensitive ratios for the 201.13 Å and 204.95 Å lines does not allow to determine which of these lines is responsible for the low value of the 201.13/204.95 ratio. As suggested by Young et al. (1998), a possible source of additional intensity to the 204.95 Å might come from an unidentified first order line at around 409.90 Å.

The 200.02/209.67 and 204.26/200.02 line ratios agree with their predicted values, suggesting that these lines have no problems. It is interesting to see that there is a significant disagreement between the SERTS-95 and the SERTS-89 line ratios involving the 209.67 Å line, and in general better agreement with observations is obtained with the SERTS-95 measurements, while some problem seems to affect the SERTS-89 value. The weakly density sensitive ratios between the 203.82 Å doublet and the 200.02 Å and 204.26 Å lines indicate that the observed intensity of the 203.82 Å doublet is slightly higher than predicted, although the FAWCETT dataset is in better agreement than the TAYAL one. A possible blend for the 203.82 Å line is rather unlikely, as the intensity of the blending line should be rather large in order to affect the total intensity of this spectral feature, and no candidate is found in CHIANTI or in other line lists for such a strong blending line. The 216.9 Å doublet is reported to be blended with a Si VIII transition and thus it is expected to be too intense, but ratios involving this doublet are much lower than predicted, showing the the 216.9 Å line intensity is too low. However, the 216.9 Å doublet looks very weak in the SERTS-95 spectrum (Fig. 1 in Brosius et al. 1998) and its observed intensity should be taken with caution.

Table 4 displays the density sensitive ratios. It is possible to see that the 200.02 Å, 202.04 Å, 203.16 Å and 209.67 Å lines, whose branching ratios and density insensitive ratios give no problem, provide very similar density

Table 3. Branching ratios and weakly density sensitive ratios for the $3s^2 3p^2$–$3s^2 3p3d$ transitions. Only some of the weakly density sensitive ratios have been reported. The TAYAL 209.67/204.26 theoretical ratio is density sensitive and is not reported here. *: The 203.80 Å and the 203.83 Å theoretical line intensities have been summed together. **: The 216.83 Å and the 216.87 Å theoretical line intensities have been summed together.

Ratio	SERTS-95	SERTS-89	TAYAL	FAWCETT
		Branching Ratios		
204.26/221.81	0.89 ± 0.19	0.93 ± 0.39	0.55	
209.67/213.76	2.29 ± 0.63	1.61 ± 1.17	1.01	
209.92/202.04	0.186 ± 0.042		0.170	
201.13/204.95	1.76 ± 0.37	1.13 ± 0.50	3.42	
		Weakly density sensitive ratios		
209.67/221.81	0.96 ± 0.21	0.62 ± 0.39	0.69 ± 0.16	0.60 ± 0.04
213.76/200.02	0.30 ± 0.08		0.74 ± 0.07	0.80 ± 0.07
209.67/200.02	0.74 ± 0.17		0.75 ± 0.07	0.81 ± 0.07
$216.9^{\star\star}/209.67$	0.26 ± 0.09		0.42 ± 0.04	0.41 ± 0.04
$209.67/203.82^\star$	0.11 ± 0.02	0.088 ± 0.050	0.16 ± 0.01	0.16 ± 0.01
209.67/204.26	1.08 ± 0.24	0.66 ± 0.41	1.26 ± 0.29	1.09 ± 0.08
213.76/204.26	0.47 ± 0.13	0.41 ± 0.23	1.24 ± 0.29	1.07 ± 0.08
204.26/200.02	0.64 ± 0.12		0.64 ± 0.19	0.76 ± 0.11
$213.76/203.82^\star$	0.048 ± 0.012	0.055 ± 0.028	0.16 ± 0.01	0.15 ± 0.01
$200.02/203.82^\star$	0.16 ± 0.03		0.22 ± 0.01	0.19 ± 0.01
$216.9^{\star\star}/203.82^\star$	0.028 ± 0.009		0.068 ± 0.002	0.064 ± 0.001

Table 4. Density sensitive ratios for the $3s^2 3p^2$–$3s^2 3p3d$ transitions.

Ratio	SERTS-95	Log N_e^{TAYAL}	Log $N_e^{FAWCETT}$	SERTS-89	Log N_e^{TAYAL}	Log $N_e^{FAWCETT}$
200.02/202.04	0.25 ± 0.04	9.14 ± 0.10	9.46 ± 0.16			
$202.04/203.82^\star$	0.63 ± 0.11	9.34 ± 0.12	9.58 ± 0.13	0.61 ± 0.14	9.36 ± 0.15	9.60 ± 0.17
204.26/202.04	0.16 ± 0.03	9.42 ± 0.12	9.51 ± 0.12	0.22 ± 0.07	9.62 ± 0.22	9.75 ± 0.25
209.62/202.04	0.17 ± 0.03	9.16 ± 0.10	9.43 ± 0.11	0.15 ± 0.08	$9.10^{+0.3}_{-0.4}$	$9.35^{+0.3}_{-0.45}$
196.54/202.04	0.11 ± 0.03	9.23 ± 0.10	9.38 ± 0.10			
203.16/202.04	0.13 ± 0.02	9.17 ± 0.10	9.49 ± 0.12			
201.13/202.04	0.39 ± 0.07	9.70 ± 0.30	9.67 ± 0.18	0.61 ± 0.24	$N_e > 9.60$	$N_e > 9.60$
221.81/202.04	0.18 ± 0.03	9.15 ± 0.09	9.22 ± 0.10	0.24 ± 0.08	9.31 ± 0.20	9.40 ± 0.20
$201.13/203.82^\star$	0.24 ± 0.04	9.16 ± 0.13	$9.4^{+0.7}_{-0.3}$	0.37 ± 0.14	$8.95^{+0.4}_{-0.2}$	$8.8^{+0.7}_{-0.3}$
$204.95/203.82^\star$	0.14 ± 0.03	8.75 ± 0.12	8.56 ± 0.20	0.33 ± 0.10	8.30 ± 0.15	8.00 ± 0.20
204.95/209.62	1.27 ± 0.29	8.55 ± 0.12	8.32 ± 0.20			

values, within each theoretical dataset. However, it is important to note that the density values measured with the FAWCETT and TAYAL datasets are significantly different. All ratios involving the 204.95 Å line provide too low densities, showing that the observed intensity of this line is too large. Results for the other lines are different in the TAYAL and FAWCETT datasets. TAYAL ratios show that the 221.81 Å and 196.52 Å lines provide densities in line with the other ratios, while problems are found for the 204.26 Å and 201.12 Å lines, giving too high densities. Also, the electron density measured by the 202.04/203.82 ratio is slightly higher than the other values. Densities for the other ratios cluster around $\log N_e \simeq 9.20$, in close agreement with the results reported in Table 2 for other ions. FAWCETT results are different for several lines. Ratios involving the 203.82 Å and the 204.26 Å lines provide densities in line with the rest of the ratios, while the 221.81 Å and 196.52 Å lines give lower values. The 201.12 Å line still provides a high density value, but the difference from the others is within the uncertainties. Overall, FAWCETT ratios give electron densities around $\log N_e \simeq 9.50$, slightly higher than the values resulting from the TAYAL dataset and the other ions.

From these observations only, it is not easy to understand which theoretical dataset is more reliable, as there is a class of lines consistent among themselves, and a few more for which the TAYAL and FAWCETT results are different. It is to be noted that TAYAL densities are slightly lower than those given by the other ions formed at temperatures close to the Fe XIII maximum abundance temperature, while FAWCETT values tend to be slightly higher. However, given the uncertainties of densities measured in the present study and those reported in Table 2, neither the TAYAL nor the FAWCETT dataset provide densities in disagreement with the values obtained with other ions, so that no clear conclusion can be drawn on which dataset is to be preferred. This is true expecially for the SERTS-95 results, which are considered more reliable for the $3s^2 3p3d$ lines, since the SERTS-89 calibration for second order lines is rather uncertain.

In light of these results, it is also possible to select a set of lines for which both datasets are consistent with each other and show no problems, and another set of lines whose problems are greater than any uncertainty in the theoretical emissivities and observed intensities. A third set of lines includes lines for which the FAWCETT and TAYAL results are different and ambiguous:

1. Lines with no problems: 200.02, 202.04, 203.16, 209.67 (SERTS-95), 209.92;
2. Lines with problems: 204.95, 209.67 (SERTS-89), 213.76, 216.90;
3. Ambiguous lines: 196.54, 201.13, 203.82, 204.26, 221.81.

It is to be noted that the 213.76 Å, 216.90 Å and the 221.81 Å observed line intensities seem to be lower than predicted by both theoretical datasets. This might also point out to some inaccuracies in the intensity calibration of the high-wavelength range of the SERTS-95 intensity calibration. Brosius et al. (1998) determined the relative intensity calibration of the SERTS-95 dataset by comparing theoretical and observed ratios from lines of all the ions present in the dataset. In particular, the 210–223 Å wavelength range calibration was determined using lines from Fe XII and Fe XIV. The agreement of the lines from these two ions seems to confirm the validity of the SERTS-95 intensity calibration, so that the discrepancies found among the Fe XIII lines in the present work are due to atomic physics problems.

4.2. $3s3p^3$ lines

The $3s^23p^2$–$3s3p^3$ transitions are found at higher wavelengths than the $3s^23p^2$–$3s^23p3d$ ones, and they have been observed mostly during the SERTS-89 flight. Only the ^3P–^3S triplet and three more lines have been observed during the 1995 flight. Moreover, the multilayer coating adopted in SERTS-95 was optimized to enhance the second order reflectivity, but the signal-to-noise ratio for the $3s3p^3$ lines, seen at first order, was poorer than in SERTS-89. For these reasons, results from the SERTS-95 ratios are used only as a confirmation to the results of the SERTS-89 ones.

The SERTS-89 flight reported most of the ^3P–^3P and ^3P–^3D transitions and the singlets ^1D–^1D, ^1D–^1P. The only lines which have not been observed are the 303.30 Å line, blended with the far stronger Si XI 303.32 Å, and the $^3P_2$–$^3D_{1,2}$ transitions expected at 372.03 Å and 372.25 Å. The $^1D_2$–$^3D_3$ intercombination line has also been observed by SERTS-89 at 413.00 Å.

Branching ratios and weakly density sensitive ratios are displayed in Table 5. Of all the theoretical branching ratios listed in Table 5, only the SERTS-89 value of 246.19/251.94 ratio and the SERTS-95 value of the 240.69/246.19 ratio agree with the observations. In all the other cases, a discrepancy is observed. The 311.56/320.80 discrepancy is a signature of the presence of the Cr XII $3s^23p\ ^2P_{3/2}$–$3s3p^2\ ^2P_{1/2}$ line blending the 311.56 Å line. The 368.16 Å line is reported to be blended with a Cr XIII line, and this explains the slight disagreement found in Table 5; however, the contribution of Cr XII is not large, as the discrepancy is nearly as large as the ratio errorbars. No candidates for blending of the 312.17 Å and 348.18 Å lines are found, so no conclusion can be drawn from the problems encountered from their ratios. The SERTS-89 and SERTS-95 measurements of the branching ratios involving the 240.69 Å, 246.19 Å and the 251.94 Å lines show rather different results. The only conclusion we can draw is that the 240.69 Å line is too high relative to the other two lines of the triplet, as already noted by Young et al. (1998).

The density insensitive line ratios listed in Table 5 allow to make a first selection of lines. It is important to note that the TAYAL and FAWCETT datasets provide slightly different results, but these differences are within the uncertainties. Ratios mutually involving the 312.17 Å, 312.87 Å, 320.80 Å, 348.18 Å, 359.64 Å and the 413.00 Å lines show good agreement with observations, giving confidence in the accuracy of the theoretical data for these lines and in the absence of blends. Also the ratios involving the 368.16 Å line show reasonable agreement with observations, despite the presence of the Cr XIII blend. This seems to confirm that the blending line does not provide a large contribution. All the ratios involving the 311.56 Å line confirm the presence of the Cr XII blend. Only marginal agreement is found in the 321.46/348.18 and 359.83/312.17 line ratios, showing that the problems already found in the branching ratios are due to the 321.46 Å and 359.83 Å lines. Surprisingly, it appears that the observed intensities of these two lines are too small, and that their theoretical emissivities are too large. This cannot be due to blends; since this problem is found also in the branching ratios, it appears that problems are most likely to be found in the radiative transition probabilities of these lines.

Table 6 lists the density-sensitive line ratios and their comparison with observations. The density measurements reported in Table 6 should also be compared with those found in Table 4. Lines whose density insensitive ratios have no problems, provide self-consistent density measurements, since the electron density values are very similar within each theoretical dataset. The only major discrepancies lie in the ratios involving the 318.10 Å line, as they provide density values always higher than all the other lines, both with the FAWCETT and TAYAL datasets. A similar problem was found by Young et al. (1998), who discussed it in terms of possible inaccuracies in transition rates; however, since in all cases it seems that the observed intensity of the 318.10 Å line is in excess, it is also possible that an unidentified blend is the cause of this discrepancy. Ratios involving the 256.43 Å line provide density values in line with the others, although their uncertainties are greater due to a more limited density sensitivity of the theoretical ratios; these uncertainties are larger than any effect given by the blending Zn XX line reported by Thomas & Neupert (1994). Of further interest are the ratios involving the 240.69 Å, 246.19 Å and the 251.94 Å

Table 5. Branching ratios and weakly density sensitive ratios for the $3s^23p^2$–$3s3p^3$ transitions.

Ratio	SERTS-95	SERTS-89	TAYAL	FAWCETT
		Branching Ratios		
240.69/246.19	0.65 ± 0.30	0.93 ± 0.47	0.40	
240.69/251.94	0.48 ± 0.22	0.41 ± 0.18	0.21	
246.19/251.94	0.74 ± 0.20	0.44 ± 0.15	0.52	
311.56/320.80		0.24 ± 0.07	0.13	
321.46/312.17		0.38 ± 0.10	0.52	
359.83/348.18		0.18 ± 0.04	0.27	
413.00/368.16		0.047 ± 0.015	0.065	
		Weakly density sensitive ratios		
312.87/320.80		0.28 ± 0.09	0.27 ± 0.03	0.27 ± 0.04
312.87/359.64		0.32 ± 0.10	0.31 ± 0.02	0.37 ± 0.02
359.64/320.80		0.85 ± 0.15	0.89 ± 0.18	0.73 ± 0.15
311.56/359.64		0.28 ± 0.08	0.16 ± 0.02	0.20 ± 0.03
311.56/368.16		0.32 ± 0.10	0.16 ± 0.01	0.18 ± 0.01
368.16/320.80		0.74 ± 0.17	0.89 ± 0.03	0.76 ± 0.05
311.56/312.87		0.86 ± 0.34	0.51 ± 0.05	0.52 ± 0.06
312.87/368.16		0.37 ± 0.13	0.31 ± 0.05	0.36 ± 0.08
413.00/312.87		0.13 ± 0.05	0.19 ± 0.02	0.17 ± 0.03
312.17/348.18		0.67 ± 0.13	0.76 ± 0.16	0.84 ± 0.21
321.46/348.18		0.26 ± 0.07	0.36 ± 0.08	0.42 ± 0.11
359.83/312.17		0.26 ± 0.06	0.37 ± 0.10	0.35 ± 0.13
359.83/321.46		0.68 ± 0.20	0.73 ± 0.21	0.69 ± 0.25

Table 6. Density sensitive ratios for the $3s^23p^2$–$3s3p^3$ transitions. *Exp. low*: the experimental ratio is always lower than predicted; *Exp. high*: the experimental ratio is always higher than predicted.

Ratio	SERTS-95	Log N_e^{TAYAL}	Log $N_e^{FAWCETT}$	SERTS-89	Log N_e^{TAYAL}	Log $N_e^{FAWCETT}$
312.87/348.18				0.37 ± 0.12	9.34 ± 0.30	9.52 ± 0.28
348.18/320.80				0.74 ± 0.13	9.42 ± 0.14	9.54 ± 0.13
348.18/359.64				0.87 ± 0.14	9.37 ± 0.15	9.68 ± 0.16
348.18/368.16				1.00 ± 0.22	9.34 ± 0.15	9.56 ± 0.16
413.00/348.18				0.047 ± 0.014	9.20 ± 0.20	9.42 ± 0.19
312.17/320.80	0.88 ± 0.31	$8.90^{+0.4}_{-0.2}$	$9.05^{+0.4}_{-0.2}$	0.50 ± 0.10	$9.38^{+0.3}_{-0.2}$	$9.56^{+0.4}_{-0.2}$
312.17/368.16				0.67 ± 0.16	$9.27^{+0.3}_{-0.2}$	$9.60^{+0.4}_{-0.2}$
413.00/312.17				0.070 ± 0.021	9.07 ± 0.25	9.37 ± 0.27
312.17/256.43				0.65 ± 0.26	$9.38^{+0.5}_{-0.4}$	$9.60^{+0.5}_{-0.3}$
348.18/256.43				0.96 ± 0.39	$9.42^{+0.4}_{-0.2}$	$9.57^{+0.3}_{-0.2}$
318.10/348.18				0.75 ± 0.14	9.61 ± 0.10	9.88 ± 0.10
318.10/320.80	0.57 ± 0.28	$9.90^{+0.5}_{-0.9}$	$10.30^{+0.5}_{-0.6}$	0.56 ± 0.11	9.90 ± 0.25	10.20 ± 0.20
240.69/320.80	0.82 ± 0.42	≥8.75	≥8.90	0.86 ± 0.37	≥8.70	≥8.90
246.19/320.80	1.26 ± 0.45	≥9.55	≥9.75	0.93 ± 0.30	Exp. low	Exp. low
320.80/251.94	0.59 ± 0.21	Exp. high	Exp. high	0.47 ± 0.09	Exp. high	Exp. high

lines, in light of the problems found with their branching ratios. Surprisingly, the 240.69 Å line, the only one that unambiguously seemed to have problems, is the only one that provides density values in line with the rest of the other ratios. The other two lines provide too low density values, revealing that their experimental intensities are weaker than predicted. This rules out the presence of blends, and seems to point towards inaccuracies of the atomic data. However, it is also possible that the apparent agreement of the 240.69 Å line is misleading, as this line is emitted by the same upper level of the other two, so that problems in the population of the upper level should be reflected in its emissivity as well. If this is the case, then it is possible that this line is also blended by an unidentified line, with the additional intensity covering the difference and causing the apparent agreement with the other $3s3p^3$ lines.

As with the $3s^23p^2$–$3s^23p3d$ transitions, the FAWCETT and TAYAL datasets provide different values of the electron density. For the SERTS-89 data, the average TAYAL electron density is around Log $N_e \simeq 9.30$, and the FAWCETT values clusters around Log $N_e \simeq 9.55$. The FAWCETT density value is in excellent agreement with the value measured with the $3s^23p^2$ – $3s^23p3d$ transitions, and the TAYAL one agrees with them within the errorbars.

Table 7. $3s3p^3/3s^23p3d$ moderately density sensitive ratios. [1]: The 203.80 Å and the 203.83 Å theoretical line intensities have been summed together.

Ratio	SERTS-89	Log N_e^{TAYAL}	Log $N_e^{FAWCETT}$	SERTS-95	Log N_e^{TAYAL}	Log $N_e^{FAWCETT}$
348.18/202.04	0.20 ± 0.04	>9.75	Exp. high			
209.62/320.80				1.08 ± 0.36	<10.7	<10.4
203.16/320.80				0.79 ± 0.26	>8.70	>8.85
256.43/203.82[1]	0.13 ± 0.05	$10.3^{+0.6}_{-1.0}$	$10.6^{+0.7}_{-2.0}$			
312.87/203.82[1]	0.045 ± 0.015	$8.5^{+1.4}_{-0.6}$	$7.9^{+1.6}_{-1.1}$			
320.80/203.82[1]	0.16 ± 0.03	$8.15^{+0.4}_{-0.2}$	$7.4^{+0.4}_{-0.3}$	0.10 ± 0.03	>8.50	>7.80
359.64/203.82[1]	0.14 ± 0.03	$8.7^{+0.4}_{-0.3}$	$8.1^{+0.4}_{-0.2}$			
413.00/203.82[1]	0.0057 ± 0.0017	>8.30	Any N_e			
256.43/204.26	0.94 ± 0.45	>8.70	>8.40			
204.26/320.80	0.82 ± 0.26	$9.6^{+0.8}_{-1.6}$	$7.3^{+2.3}_{-0.7}$	1.00 ± 0.33	$10.2^{+0.7}_{-1.9}$	$7.7^{+2.9}_{-0.7}$
413.00/204.26	0.043 ± 0.017	>9.55	Any N_e			
256.43/201.12	0.34 ± 0.17	<9.50	<10.2			
312.17/201.12	0.22 ± 0.08	<9.70	$9.7^{+1.1}_{-0.5}$	0.37 ± 0.09	>8.10	$8.9^{+0.4}_{-0.3}$
348.18/201.12	0.32 ± 0.12	>9.50	$9.6^{+0.7}_{-0.3}$			
413.00/201.12	0.015 ± 0.007	8.85 ± 0.35	$9.1^{+0.9}_{-0.6}$			
320.80/201.12	0.44 ± 0.16	9.1 ± 0.3	>8.75	0.41 ± 0.13	9.05 ± 0.25	>8.75
312.87/201.12	0.12 ± 0.05	8.95 ± 0.35	9.1 ± 0.65			
359.64/201.12	0.37 ± 0.14	8.95 ± 0.40	>8.60			
240.69/209.62				0.76 ± 0.34	$9.0^{+1.7}_{-0.3}$	$9.1^{+1.6}_{-0.3}$
240.69/203.16				1.04 ± 0.46	$8.9^{+0.8}_{-0.3}$	$9.1^{+1.9}_{-0.4}$
240.69/201.12	0.38 ± 0.20	Any N_e	>8.00	0.34 ± 0.15	<9.6	>8.4
320.80/196.52				1.44 ± 0.56	9.15 ± 0.45	9.00 ± 0.1

Table 8. $3s3p^3/3s^23p3d$ strongly density sensitive ratios. [1]: The 203.80 Å and the 203.83 Å theoretical line intensities have been summed together.

Ratio	SERTS-89	Log N_e^{TAYAL}	Log $N_e^{FAWCETT}$	SERTS-95	Log N_e^{TAYAL}	Log $N_e^{FAWCETT}$
348.18/203.16	0.91 ± 0.29	$9.30^{+0.4}_{-0.2}$	$9.5^{+0.4}_{-0.2}$			
320.80/202.04	0.27 ± 0.06	9.60 ± 0.2	$10.0^{+0.4}_{-0.3}$	0.16 ± 0.05	9.25 ± 0.2	9.55 ± 0.2
413.00/202.04	0.0093 ± 0.0029	9.40 ± 0.2	9.8 ± 0.25			
312.87/202.04	0.074 ± 0.025	9.60 ± 0.3	$10.1^{+1.4}_{-0.5}$			
359.64/202.04	0.23 ± 0.05	9.60 ± 0.2	10.7 ± 0.7			
209.62/312.17				1.22 ± 0.31	8.80 ± 0.15	8.90 ± 0.15
203.16/312.17				0.90 ± 0.23	8.70 ± 0.15	8.90 ± 0.2
312.17/203.82[1]	0.081 ± 0.017	9.05 ± 0.15	9.15 ± 0.2	0.089 ± 0.021	9.00 ± 0.15	9.10 ± 0.2
312.17/204.26	0.61 ± 0.20	$9.40^{+0.45}_{-0.25}$	$9.30^{+0.45}_{-0.2}$	0.88 ± 0.22	$9.10^{+0.25}_{-0.15}$	9.00 ± 0.2
196.52/312.17				0.78 ± 0.25	9.00 ± 0.15	9.10 ± 0.15

SERTS-95 line ratios show higher uncertainties, but confirm the SERTS-89 results. However, it is to be noted that the observed intensities of the 312.17 Å and 246.19 Å lines seem to be higher than their SERTS-89 values, relatively to the other Fe XIII lines, although the uncertainties are as large as the differences themselves.

In light of these results, it is possible to select a set of lines for which both dataset are consistent with each other and show no problems, and another set of lines whose problems are greater than any uncertainty given by the theoretical emissivities. A third set of lines includes those for which the FAWCETT and TAYAL results are ambiguous:

1. Lines with no problems: 256.43, 312.17, 312.87, 320.80, 348.18, 359.64, 368.16 (small blend), 413.00;
2. Lines with problems: 246.19, 251.94, 311.56, 318.10, 321.46, 359.83;
3. Ambiguous lines: 240.69.

4.3. $3s^2\,3p3d$ versus $3s3p^3$ lines

The comparison between $3s^23p3d$ and $3s3p^3$ lines has been carried out using the lines listed as reliable in Sects. 4.1 and 4.2. Also, a few ambiguous lines have considered as well, to further investigate. The relative density sensitivity of lines coming from these two configurations is such that there are no strictly density insensitive line ratios. However, there are a few intensity ratios that are only moderately density sensitive, and they are listed in Table 7. Table 8 reports the more strongly density sensitive ratios.

Since the SERTS-89 line intensities for the $3s^2 3p3d$ transitions are more uncertain than the SERTS-95 measurements, we will take the SERTS-95 results as more reliable, while SERTS-89 will only be used to confirm them. For the many $3s3p^3$ lines not present in the SERTS-95 dataset, SERTS-89 results will be discussed.

The moderately density sensitive ratios in the SERTS-95 dataset show a remarkable good agreement between theoretical predictions and observations, whichever theoretical dataset is used. The only exceptions are given by the 312.17/201.12 and 320.80/196.52 ratios, showing agreement only if they are calculated with the TAYAL dataset. It is interesting to note that the 240.69 Å line is in fairly good agreement with all the others, while its ratios with lines of the $3s3p^3$ group provided ambiguous results. Ratios in Table 8 provide density measurements in agreement with the results obtained in the previous sections in only one case (320.80/202.04). In all other cases, problems arise only with the 312.17 Å line both with the TAYAL and FAWCETT datasets: measured densities are always lower than expected in all cases, the disagreement being worse with FAWCETT ratios than with the TAYAL ones.

Results obtained with the SERTS-89 dataset are more ambiguous. Moderately density sensitive line ratios show that the 201.12 Å, 204.26 Å, 240.69 Å, 256.43, 312.17 Å and 359.64 Å lines do not present particular problems, while it is not easy to understand the behaviour of the remaining lines, especially the strong 203.82 Å line, as in some cases their ratios agree with observations, and in others they do not. Also, The 348.18/202.04 ratio is the only one involving these two lines, and it is not possible to understand which line is responsible for the disagreement reported in Table 7.

No help comes from the strongly density sensitive ratios. A few of them provide electron densities in agreement with the measurements carried out in the previous sections, while in other cases problems arise. In general, it is not possible to draw any conclusion for the few lines (312.87 Å, 348.18 Å, 359.64 Å and 413.00 Å) for which no data are available in the SERTS-95 dataset. Only the 256.43 Å line provides ratios in agreement with observations.

In general, there is no trace of the systematic disagreement found by Landi & Landini (1997). Their result was possibly due to the fact that they used a subset of the SERTS-89 observation, whose signal-to-noise ratio was even poorer than that of the SERTS-89 dataset used here.

Considering the higher uncertainties in the SERTS-89 fluxes, the only results we can draw is that the lines whose intensities were observed by SERTS-95 and considered reliable in the previous sections, have no problems. The only exceptions is the 196.52 Å transition, for which only the TAYAL dataset is able to provide reasonable agreement between theory and observations, and with results obtained in the previous sections.

Table 9. Fe XIII lines recommended for plasma diagnostics. Group A line intensities increase as the electron density increases, group B line intensities decrease as the electron density increases. *: contradictory results are found in $3s3p^3/3s^2 3p3d$ ratios.

Group	Selected Line
A	200.02, 203.16, 209.67
	201.13, 203.82*
	256.43, 312.87*, 320.80
	359.64*, 413.00*
B	202.04, 209.92
	312.17*, 348.18*

4.4. Lines recommended for plasma diagnostic studies

Lines that were found to have no problems are reported in Table 9. A few more lines are listed, for which ambiguous results were found; these are marked with "$\star$". The recommended lines are listed according to the behaviour of their predicted emissivity versus the electron density. Emissivities of lines of group A increase as the electron density increases; on the contrary, those of lines of group B decrease. Thus, any given line pair involving one line from each group can be used for density diagnostics on any plasma hot enough to emit Fe XIII lines. Ratios of lines belonging to the same group have a limited, if any, dependence on the electron density. The latter ratios can be used for instrument calibration, according to the methods used by Neupert & Kastner (1983) and Del Zanna et al. (2001). Both the TAYAL and FAWCETT datasets provide the same set of reliable lines, so that this selection is not biased by the choice of theoretical dataset.

5. Conclusions

In the present work Fe XIII line intensities observed with the SERTS instrument in 1989 and 1995 have been compared with theoretical estimates of emissivities obtained by using two different datasets of atomic data and transition rates.

Differencies in line emissivities and in line ratios calculated using the TAYAL and FAWCETT datasets are rather large, and can rise up to a factor 2.5. These differences depend on both the electron density and temperature, and therefore will have a significant impact on the diagnostics results obtained through the use of Fe XIII lines.

The comparison with observations has shown that the TAYAL and FAWCETT datasets provide different results in terms of plasma diagnostics. Also, the use of each dataset leads to a set of measured self-consistent electron densities. The differences in the theoretical emissivities between the two datasets, briefly outlined in Sect. 2, show their effects in the values of the electron densities they allow to measure. Infact, TAYAL-based densities are on the average smaller than the FAWCETT results by a factor around 2, at the limit of the experimental uncertainties. Also, the analysis on the SERTS-95 ratios between

$3s^2 3p3d$ and $3s3p^3$ lines has shown that in a few cases the TAYAL dataset allows a better agreement with the observations than the FAWCETT one.

The comparison between the densities measured with the two theoretical datasets and results obtained by line ratios from other ions formed at temperatures close to Fe XIII maximum abundance temperature does not allow a definitive conclusion on which dataset is more reliable. The SERTS-95 plasma density seems to be around Log N_e = 9.4, and the SERTS-89 value is around Log N_e = 9.3, closer to the TAYAL values. However, the uncertainties associated with the present measurements, as well as the scatter of the density values provided by line ratios from other ions reported in Table 2, are of the same magnitude of the differences between the TAYAL and FAWCETT results, so that a definitive conclusion cannot be reached on which of the two theoretical datasets is to be preferred.

The present study has also made possible a selection of lines which have proved to be free of blending and atomic physic problems; these are reported in Table 9.

A few remaining disagreements between predicted emissivities and observed line intensities indicate that further calculations of atomic structure and transition rates are still needed.

Acknowledgements. This work has been supported by a grant from NASA's Applied Informations System Research Program (AISRP), and by the Max-Planck-Gesellschaft. The author gratefully acknowledges very useful comments and discussions with Prof. Massimo Landini and Dr. Uri Feldman, and valuable comments from the referee.

References

Binello, A. M., Landi, E., Mason, H. E., Storey, P. J., & Brosius, J. W. 2001, A&A, 370, 1071
Brickhouse, N. S., Raymond, J. C., & Smith, B. W. 1995, ApJSS, 97, 551
Brosius, J. W., Davila, J. M., Thomas, R. J., & Monsignori Fossi, B. C. 1996, ApJS, 106, 143
Brosius, J. W., Davila, J. M., & Thomas, R. J. 1998, ApJSS, 119, 255
Brosius, J. W., Thomas, R. J., Davila, J. M., & Landi, E. 2000, ApJ, 543, 1016
Cowan, R. D. 1981, The theory of atomic spectra (Univ. of California Press, Los Angeles)
Del Zanna, G., Bromage, B. J. I., Landi, E., & Landini, M. 2001, A&A, 379, 708
Dere, K. P. 1982, Sol. Phys., 77, 77
Dere, K. P., Mason, H. E., Widing, K. G., & Bhatia, A. K. 1979, ApJS, 40, 341
Dere, K. P., Landi, E., Mason, H. E., Monsignori Fossi, B. C., & Young, P. R. 1997, A&AS, 125, 149
Dere, K. P., Landi, E., Young, P. R., & Del Zanna, G. 2001, ApJS, 134, 331
Eissner, W., & Seaton, M. J. 1972, J. Phys. B., 5, 2187
Eissner, W., Jones, M., & Nussbaumer, H. 1974, Comp. Phys. Comm., 8, 230
Fawcett, B. C. 1987, Rutherford Appleton Laboratory report RAL-87-051
Fawcett, B. C., & Mason, H. E. 1989, ADNDT, 43, 245
Flower, D. R. 1971, J. Phys. B., 4, 697
Flower, D. R., & Pineau des Forêts, G. 1973, A&A, 24, 181
Flower, D. R., & Nussbaumer, H. 1974, A&A, 31, 353
Gupta, G. P., & Tayal, S. S. 1998, ApJ, 506, 464
Keenan, F. P., Foster, V. J., Drake, J. J., Tayal, S. S., & Widing, K. G. 1995, ApJ, 453, 906
Landi, E., & Landini, M. 1997, A&A, 327, 1230
Landi, E., & Landini, M. 1998, A&A, 340, 265
Mason, H. E. 1994, ADNDT, 57, 305
Mason, H. E., Landi, E., Pike, C. D., & Young, P. R. 1999, Sol. Phys., 189, 129
Mazzotta, P., Mazzitelli, G., Colafrancesco, S., & Vittorio, N. 1998, A&ASS, 133, 403
Neupert, W. M., & Kastner, S. O. 1983, A&A, 128, 181
O'Shea, E., Doyle, J. G., & Keenan, F. P. 1998, A&A, 338, 1102
Storey, P. J., Mason, H. E., & Young, P. R. 2000, A&AS, 141, 285
Tayal, S. S. 1995, ApJ, 446, 895
Tayal, S. S. 2000, ApJ, 544, 575
Thomas, R. J., & Neupert, W. M. 1994, ApJSS, 91, 461
Young, P. R., Landi, E., & Thomas, R. J. 1998, A&A, 329, 291